Integrated Structural Electromagnetic Shape Control of Large Space Antenna Reflectors

S. L. Padula,* H. M. Adelman,* and M. C. Bailey†
NASA Langley Research Center, Hampton, Virginia
and
R. T. Haftka‡
Virginia Polytechnic Institute and State University, Blacksburg, Virginia

The requirements for extremely precise and powerful large space antenna reflectors have motivated the development of a procedure for static shape control of the reflector surface. A mathematical optimization procedure has been developed that improves antenna performance while minimizing necessary shape-correction effort. The control procedure is based on regulating electromagnetic (EM) performance in contrast to previous work, which is based on controlling the rms distortion error of the surface, thereby indirectly improving antenna performance. The application of the control procedure to a radiometer design with a tetrahedral truss backup structure demonstrates the potential for significant improvement. The results indicate the benefit of including EM performance calculations in procedures for shape control of large space antenna reflectors.

Nomenclature

G	= maximum power density (gain) for distorted antenna
G_0	= maximum power density (gain) for undistorted antenna
m	= number of shape-control actuator locations
n	= number of joints between truss elements on reflector surface
rms	= root mean square of surface distortion errors
SLL	= maximum power density outside the main beam radiation angle (side lobe level)
U	= influence matrix used in Eq. (1)
X,Y,Z	= Cartesian coordinate system with origin at center of paraboloid (Fig. 1)
z	= vector of n surface displacement errors in Z direction
β	= slack variable used to implement optimization procedure
Δl	= vector of actuator length changes
Δl_{max}	= maximum change in actuator length
θ	= antenna radiation angle measured from the paraboloid axis
θ_0	= radiation angle that defines main beam region
λ	= wavelength of electromagnetic radiation
ϕ	= azimuthal angle measuring rotation around the paraboloid axis
ψ	= vector of random surface displacement errors in the Z direction

Presented as Paper 87-0824 at the AIAA/ASME/ASCE/AHS Structures, Structural Dynamics, and Materials Conference, Monterey, CA, April 6–8, 1987; received May 4, 1987; revision received April 4, 1988.

*Senior Research Engineer, Interdisciplinary Research Office. Member AIAA.
†Senior Research Engineer, Guidance and Control Division.
‡Professor, Department of Aerospace and Ocean Engineering. Member AIAA.

Introduction

In the design and operation of large space antenna reflectors, a key issue is the precise shape control of the reflector surface in order to guarantee satisfactory electromagnetic (EM) performance. When discussing antenna design criteria, most authors treat the subjects of structural design, shape control, and EM performance as separate issues.[1-4] The only design criterion shared by these three is the rms value of surface distortion error. This rms distortion value can be used to calculate the gain-loss for a slightly distorted reflector antenna by using classical formulas such as that of Ruze.[5] Although gain-loss is an important measure of antenna performance, other performance parameters (i.e., beam shape, beam pointing direction, beam efficiency, maximum side lobe level, and polarization purity) are also important. The rms surface distortion error alone is not a reliable indicator for these performance measures because they depend upon the details of the distortion throughout the reflector surface.

There are several possible ways to compensate for the loss in antenna performance caused by reflector surface distortion. One approach is to modify the feed characteristics as suggested in Ref. 6. Another approach is to move the feed, since a distortion of the surface has a defocusing effect. Reference 7 derives expressions for the tilt angle and the displacement needed to maximize enclosed power (i.e., beam efficiency) for laser applications. The present paper describes a third approach, shape control of the reflector surface, as a means of optimizing performance. It is quite likely that some combination of these approaches will be necessary in order to meet the mission requirements of very large space antennas.

Recently, some initial steps essential to a shape-control optimization procedure have been taken. Several references describe integration of structural, thermal, and EM analysis in order to produce a more effective analysis procedure and to account for the relation between details of the surface distortion and antenna performance.[8-11]

The present paper proposes, develops, and demonstrates an optimization procedure for static shape control of a large space antenna (LSA) reflector. The main feature that distinguishes this work from previous efforts is that the shape is controlled so as to satisfy explicit EM design requirements rather than implicit limits on rms surface accuracy. In the present work, the radiometer surface shape is controlled by a set of actuators that can lengthen or shorten individual members of the backup structure. The optimization procedure

must select a set of actuator inputs that adjusts the shape of the reflector surface enough to satisfy EM performance criteria, while minimizing the total actuator effort required.

The optimization procedure is tested by applying it to a specific antenna configuration that was designed for a microwave radiometer mission. A radiometer design is attractive because remote sensing is a driving force behind NASA interest in LSA systems and because the requirements for electromagnetic performance are both critical and difficult to achieve.

Structural Shape Control

This section describes the application of shape control to a tetrahedral truss antenna structure similar to designs developed for NASA.[3,4] Figure 1 illustrates a typical antenna configuration and the coordinate system used to analyze the antenna performance. The support structure is a tetrahedral truss that is likely to be fabricated from graphite epoxy tubes. In the following discussion, the individual truss members are divided into three groups: those on the top or feed facing surface, those on the bottom surface, and those that connect the two surfaces.

The disturbances that affect the shape of such a space structure may be divided into two types. One type is transient, which leaves the structure unchanged once damped out. Such disturbances can be treated by enhancing the damping in the structure. The second type of disturbance is typified by fixed deformations (e.g., manufacturing errors) or those that are slowly varying and may be considered quasisteady. These latter disturbances may be offset by slowly applied, long-acting corrections. The second type of disturbance is the kind addressed by the present paper.

The principal source of distortion in the truss is expected to be due to changes in the lengths of the individual truss members. The length changes may result from manufacturing variations in material properties or length, on-orbit degradation of properties, or thermal distortions. In the present work, no attempt is made to calculate the magnitude of distortions due to the previously cited sources. Rather, a single set of random member length errors is selected and used to test the shape-control optimization procedure proposed in this study. The errors in member length are assumed to be normally distributed with a mean of zero and a standard deviation of 0.015% of element length. These errors are consistent with the studies in Ref. 12 where the statistics of the distortion field were determined by performing multiple structural analyses with multiple sets of member length errors selected at random according to an assumed probability density function.

Shape correction of the top surface of the truss structure is similar to the method described in Ref. 13. A set of m actuators is positioned on the bottom surface of the truss structure. The action of these actuators is to lengthen or shorten the individual elements to which they are attached. The best locations for the actuators are found by the method of Ref. 14.

The net surface shape distortion resulting from member length errors and actuator inputs is computed by a standard finite-element structural analysis program EAL.[15] For any set of actuator inputs, the vector of displacement errors in the Z direction of the feed facing surface can be expressed as

$$\{z\} = \{\psi\} + [U]\{\Delta l\} \tag{1}$$

where $\{\Delta l\}$ is the vector of changes in length of actuator elements, $\{\psi\}$ is the original random distortion error vector, $\{z\}$ is the distortion error after correction, and $[U]$ is an influence matrix. The influence matrix is assembled in EAL such that the ith column of $[U]$ is the displacement of the structure due to a unit length change in the ith actuator element.

Electromagnetic Characteristics

The EM analysis in this study was performed by a modified version of the NEC-REF[16] reflector antenna code. The original NEC-REF code accounts for changes in feed characteristics and reflector geometry but assumes that the reflector surface is perfectly smooth. The code was extended to model a distorted reflector surface. The accuracy of the modified NEC-REF code for predicting the radiation patterns of distorted reflector antennas has been verified[17] through comparison with measured results for two mesh reflector antennas.

The modified code accounts for the actual surface distortion predicted by the finite-element structural analysis. Using a spline interpolation routine, the values of the distortion errors in the Z direction are interpolated for points on the reflector surface that lie between the joints in the truss structure. The interpolation scheme uses a fifth-order bivariate polynomial as described in Ref. 18 and enforces continuity of first and second partial derivatives at each joint and continuity of first partial derivatives normal to each truss element. This interpolation scheme is particularly suitable for the present mesh-covered tetrahedral truss test case, as has been proved in

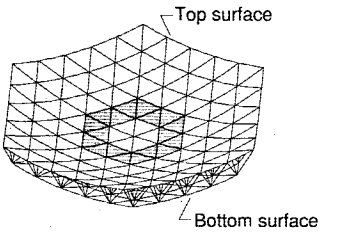

a) Reflector antenna configuration

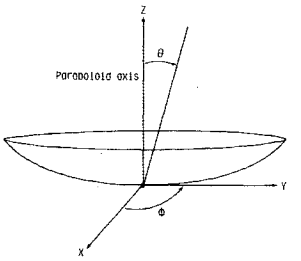

b) Cartesian and cylindrical polar coordinate systems

Fig. 1 Geometry for radiometer antenna.

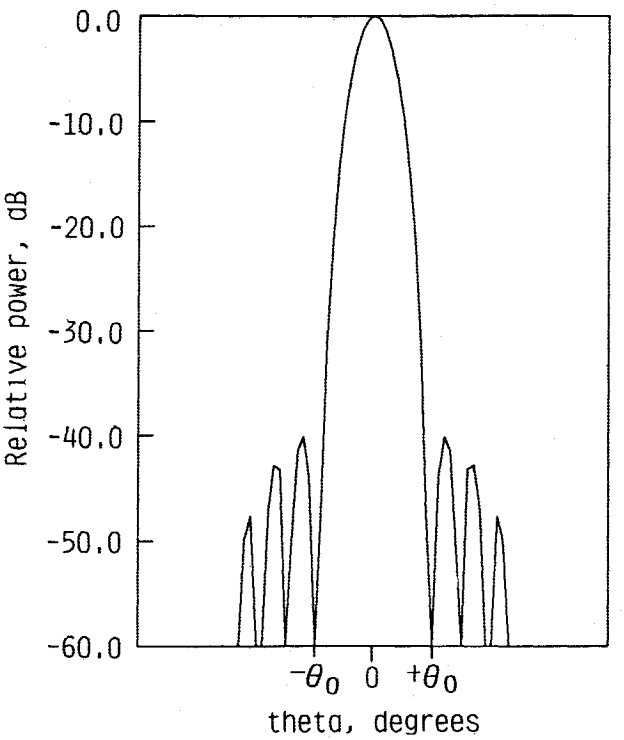

Fig. 2 Typical EM radiation patterns assuming undistorted reflector surface.

practice.[17] However, other interpolation schemes should be investigated for future applications.

The EM calculations are obtained by a geometrical optics projection of the feed radiation reflected from the antenna surface onto a plane normal to the axis of the paraboloid. The phase of these fields then is perturbed by the difference in the ray path length caused by the reflector surface distortion. A double numerical Fourier transform of these perturbed fields yields the EM characteristics of the reflector antenna.

The EM radiation characteristics for an undistorted reflector antenna are illustrated in Fig. 2 by a plot of radiated power density vs the angle θ measured from the paraboloidal axis. The plot is normalized to the maximum power density, referred to as the antenna gain G. The main beam of the antenna radiation pattern is defined by nulls that occur at $\theta = \pm\theta_0$. The maximum side lobe level (SLL) is defined as the highest level of the radiation pattern outside the main beam. The radiation pattern is axisymmetric.

Figure 3 illustrates the effect of a typical surface distortion on the radiation pattern of the antenna. Patterns for two orthogonal planes ($\theta = 45$ deg, 135 deg) are presented that illustrate that the radiation patterns from the distorted antenna are no longer axisymmetric but become a function of azimuth angle.

An antenna radiation pattern such as that illustrated in Fig. 3 is particularly detrimental to the operation of a radiometer. A radiometer interprets differences in received power at different orbital positions as differences in EM emission from the Earth, which in turn can be used to infer physical characteristics of the surface such as soil moisture or ocean salinity. The received power is an integral over all angular directions of EM emission arriving at the antenna. The emission received at each angle is weighted inside the integral by the relative power in the antenna radiation pattern for that angle. Therefore, low-side lobe levels in the radiation pattern suppress the influence of extraneous emissions. Conversely, large-side lobe levels can cause totally inaccurate readings. This happens, for example, if the radiometer is pointed at an area of low emission, but side lobes are pointed at areas of high emission.

The antenna performance parameter of most importance for a radiometer is the amount of energy within the main beam relative to the amount of energy in all other directions. The relative energy in the main beam is defined as the beam efficiency and is determined by comparing the double integral of the radiation pattern over the main beam with the double integral of the radiation pattern over 4π steradians. In an optimization procedure in which the radiation pattern changes for each step of the optimization, the numerical calculation of beam efficiency as a constraint would be prohibitively time-consuming. However, since the energy contained in the side lobe region can be a significant source of error for a radiometer system,[19] the maximum level of the radiation for angles greater than θ_0 is the primary constraint imposed in the optimization procedure. In order to further ensure that the antenna beam efficiency remains high, an additional constraint is imposed upon the decrease in maximum gain compared to the gain for the undistorted antenna G_0.

For other large antenna applications (e.g., communications and radar), the gain and SLL are the performance parameters of most importance. Therefore, constraining these parameters in the shape-control optimization procedure also will demonstrate the flexibility of the procedure for a wide class of large antenna applications. Several other antenna performance parameters (e.g., polarization purity, beam-pointing direction, and feed-positioning accuracy) will not be constrained in this present study, although these could be included in the shape-control optimization procedure for an application in which these parameters were of significant concern.

Shape-Control Optimization Formulation

In this section an optimization procedure is described that will improve the surface accuracy and the resulting EM performance of the antenna reflector, while minimizing the energy used to power the actuators. The design variables for the procedure are the actuator inputs Δl. The optimization problem is solved using the method of feasible directions as implemented in CONMIN.[20]

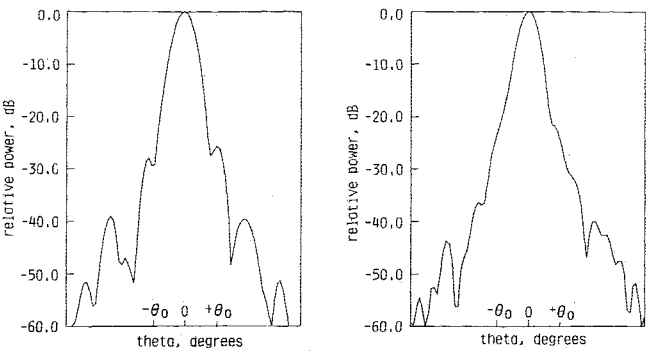

a) $\phi = 45$ deg b) $\phi = 135$ deg

Fig. 3 Typical EM radiation patterns for randomly distorted reflector surface.

The optimization procedure seeks to minimize the maximum actuator input. This objective tends to distribute the corrective force evenly among all of the actuators. Thus, actuators can be sized smaller and lighter, and the total amount of power required can be reduced.

The optimization problem is as follows:

$$\begin{aligned} &\text{minimize an objective function} && \Delta l_{\max} \\ &\text{subject to the constraints} && \text{SLL} \le G_0 - 30 \text{ dB} \\ & && G \ge G_0 - 0.3 \text{ dB} \\ & && \text{rms} \le \lambda/50 \end{aligned} \tag{2}$$

where $\Delta l_{\max}$ is the maximum change in length of an actuator (i.e., $\max_i |\Delta l_i|$) and λ the wavelength of EM radiation. The rms distortion error is defined as

$$\text{rms} = \left(\sum_{i=1}^{n} z_i^2/n\right)^{1/2} \tag{3}$$

The primary constraint on EM performance is that the maximum SLL must be at least 30 dB below the ideal antenna gain. The added constraint on antenna gain G means that at least 95% of the signal power will be in the main beam of the antenna. The final constraint (on the rms surface distortion error) is included to help the optimization routine eliminate unproductive search directions. The rms error constraint is consistent with the antenna gain constraint for small amounts of distortion.[5]

Because $\Delta l_{\max}$ is not a smooth function of the design variables, the optimization problem is formulated with a slack variable β as the objective function, thus,

$$\begin{aligned} &\text{minimize} && \beta \\ &\text{subject to} && |\Delta l_i| \le \beta, \qquad i = 1,2,\ldots,m \\ & && SLL \le G_0 - 30 \text{ dB} \\ & && G \ge G_0 - 0.3 \text{ dB} \\ & && \text{rms} \le \lambda/50 \end{aligned} \tag{4}$$

An important aspect of the optimization problem is that the EM constraints are relatively expensive to compute. Thus, the EM performance measurements and the finite-difference approximation to the gradients of the constraint functions are calculated initially. But, each time CONMIN requires a revised constraint value, linear approximations are used. The optimization problem is solved with move limits on the design variables so that the linear approximation will remain valid. When a solution is reached, the actual values of EM performance are calculated at the solution point. If this solution is a feasible one and if the objective function has not changed sig-

nificantly from the previous value, then the process stops. Otherwise, the constraint gradients are recalculated, and the entire process is repeated until an acceptable solution is found. Because a linear approximation is used for objective function and constraints, the procedure is essentially a sequential linear program (SLP).

Test Problem

The optimization procedure is applied to a specific test problem detailed in this section. The problem is constructed by selecting realistic parameter values from tables found in Refs. 3 and 4. The resulting problem has challenging performance criteria but is not a worst-case model.

The 55-m tetrahedral truss reflector, illustrated in Fig. 1, has a focal length to diameter ratio of 1.5 and an operating frequency of 1.4 GHz. The wavelength λ of EM radiation is 8.436 in. The antenna gain for the ideal antenna G_0 is 56.64 dB, and the radiation angle defining the main beam θ_0 is 0.5 deg.

The antenna backup structure is composed of 420 truss elements. The reflective surface is approximated by a spline fit through the 61 joint locations on the top surface of the antenna. The distortion at these 61 discrete points is controlled by 48 actuator elements on the bottom surface.

As discussed in the section on EM characteristics, the NECREF code calculates relative power levels at discrete values of θ and ϕ. In order to reduce the amount of computation required, SLL is defined as the maximum level found in the range $\theta_0 < |\theta| < 4\theta_0$ for four different values of ϕ that are 45 deg apart. It is assumed that an antenna surface that reduces the SLL in these four directions will reduce levels in all directions. The constraints on loss of antenna gain and on rms error are added insurance that SLL will decrease in all directions. The consequences of this assumption are discussed in a later section.

Results

Figure 4 contains a convergence history of the test optimization problem. Starting with zero inputs (i.e., $\Delta l_i = 0$), the optimization procedure converges to a feasible set of inputs that has the lowest possible $\Delta l_{\max}$. The entire process requires 11 optimization cycles, i.e., 11 evaluations of the EM performance measures and their gradients. Figure 4a is a plot of the objective function $\Delta l_{\max}$ as a function of optimization cycle number. The maximum actuator input increases until a feasible design is reached and then decreases smoothly to a final value of 0.066 in.

As seen in Figs. 4b and 4c, the requirement for low-side lobe levels is met after seven optimization cycles, but the requirement for increased gain is met in only one cycle. The final solution has a maximum SLL just slightly above the dashed line, which represents the limiting level of $G_0 - 30$ dB. The procedure will tolerate a moderate amount of constraint violation.

In terms of expansion or contraction of individual truss elements, a change in length of 0.066 in. seems very small. However, as seen in Fig. 4d, these small changes in length are enough to reduce the rms surface error from a starting value of 0.42 in. to a final value of $\lambda/50 = 0.17$ in. and to produce a significant improvement in EM performance.

Figure 5 illustrates the change in antenna radiation patterns as a result of the optimization procedure. Figure 5 represents relative power as a function of θ for two selected values of ϕ. The final patterns are shaded black so that they may be compared to the original patterns that are white. The dashed line indicates the acceptable limit on SLL. The SLL are reduced for most values of θ and ϕ, but the most significant effect of the optimization procedure is to narrow the main beam. It is anticipated that this amount of improvement in EM performance will have a significant effect on the accuracy of radiometer measurements.

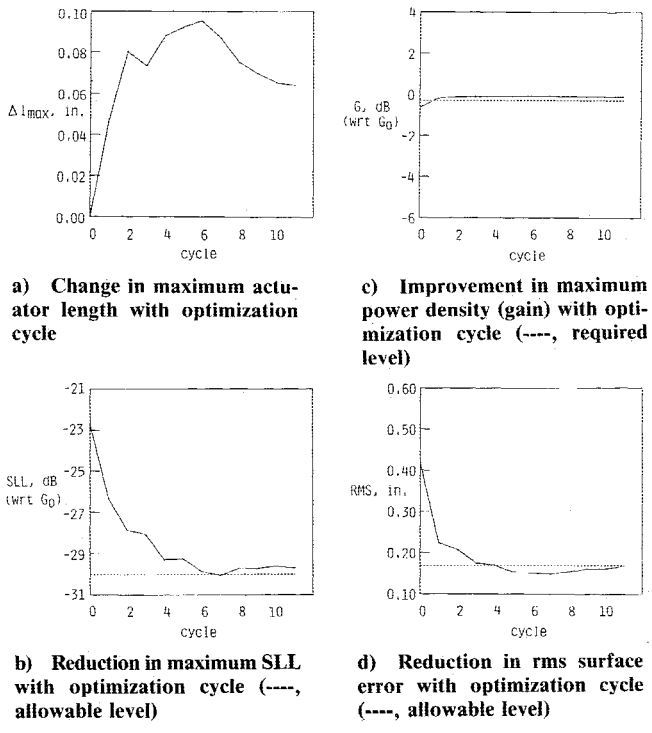

a) Change in maximum actuator length with optimization cycle

c) Improvement in maximum power density (gain) with optimization cycle (----, required level)

b) Reduction in maximum SLL with optimization cycle (----, allowable level)

d) Reduction in rms surface error with optimization cycle (----, allowable level)

Fig. 4 Convergence history of the optimization procedure.

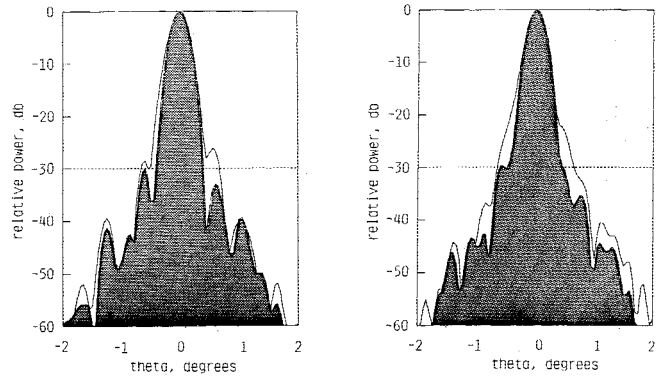

a) $\phi = 45$ deg b) $\phi = 135$ deg

Fig. 5 Comparison of EM radiation patterns before (white) and after (dark) full optimization (----, allowable SLL).

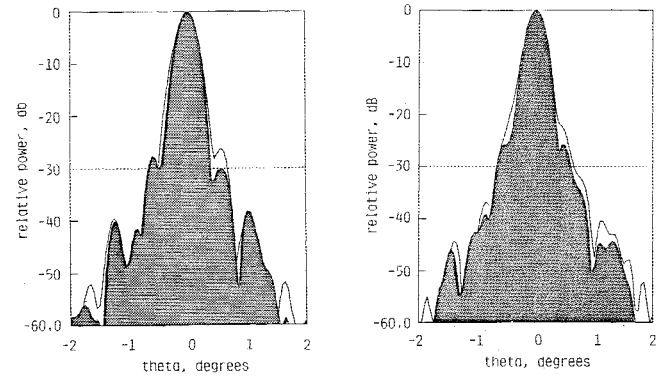

a) $\phi = 45$ deg b) $\phi = 135$ deg

Fig. 6 Comparison of EM radiation patterns before (white) and after (dark) rms-limited optimization (----, allowable SLL).

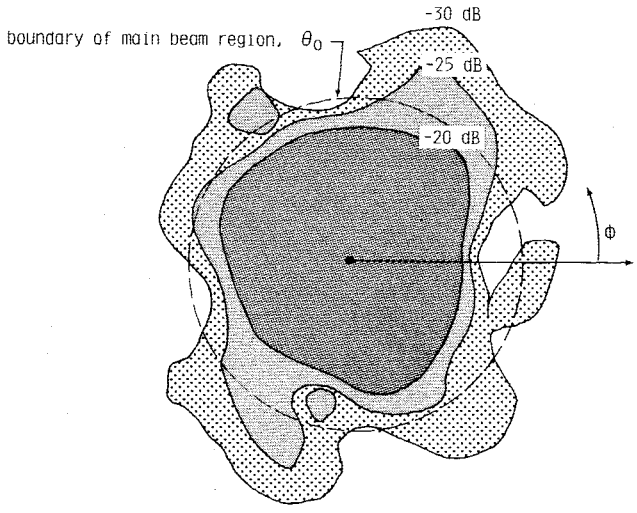

a) Power level contours before optimization

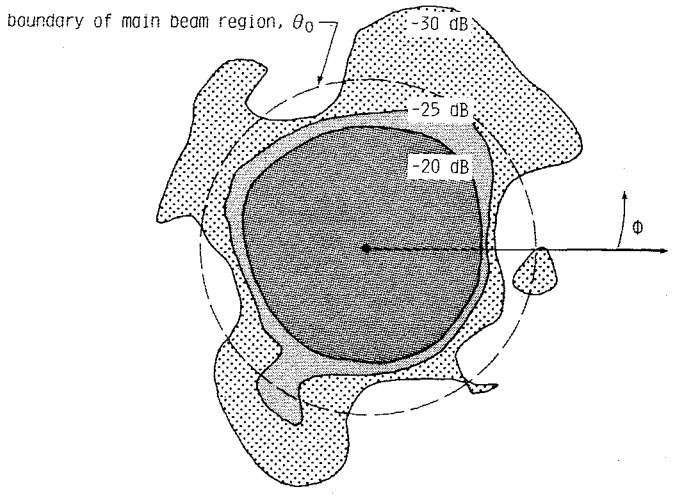

c) Power level contours after rms-limited optimization

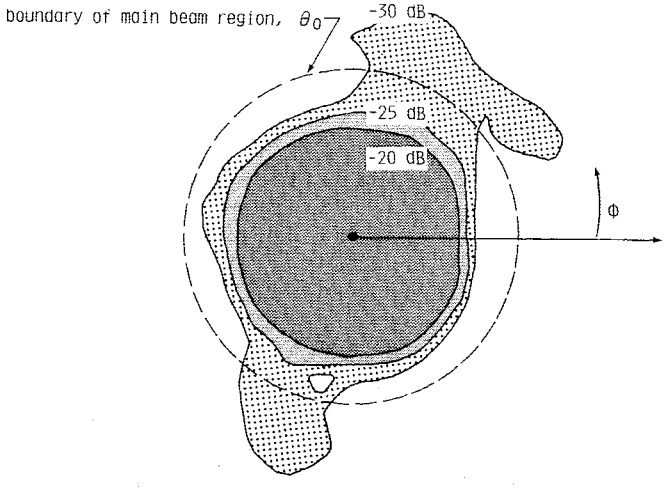

b) Power level contours after full optimization

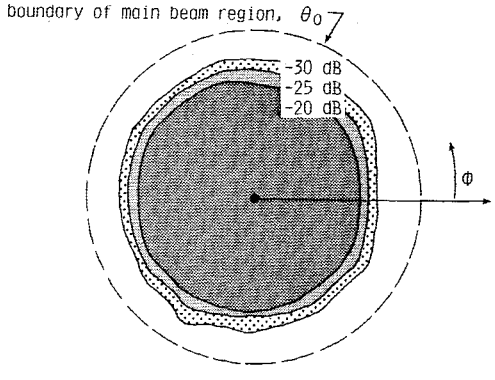

d) Power level contours for minimum rms surface distortion

Fig. 7 Predicted relative power levels on any plane normal to paraboloid axis.

Alternate Methods of Shape Control

The conventional approach to antenna shape control (e.g., Ref. 3) is to use rms surface error as the sole criterion for improvement in the reflector surface geometry. In this section, the advantages and disadvantages of including EM performance criteria are explored.

The control optimization procedure can be repeated easily without EM calculations as

$$\text{minimize} \quad \beta$$

$$\text{subject to} \quad \text{rms} \leq \lambda/50 \quad \text{and} \quad |\Delta l_i| \leq \beta, \quad i = 1,2,\ldots,m \tag{5}$$

This optimization problem can be solved very quickly because evaluation of Eq. (3) for the rms distortion is trivial compared to evaluating antenna performance. Figure 6 compares the antenna patterns for azimuthal angles $\phi = 45$ and 135 deg produced by the rms-limited procedure with the antenna patterns of the uncorrected antenna. Notice that there is very little improvement and that many of the SLL exceed the limiting value. Clearly, simply reducing the rms surface error does not guarantee acceptable antenna performance. On the other hand, Fig. 4 indicates that the full optimization procedure reduces rms first and then satisfies side lobe limits. This suggests that the rms-limited procedure may provide an efficient way to calculate a good initial guess at the solution set possibly leading to faster convergence.

Another possible solution to antenna shape control is to strictly minimize rms error without regard to actuator cost. There is a set of actuator inputs that minimize $z^T z$ and that therefore produce the minimum rms distortion.[13] This set, $\{\Delta l\}$, satisfies the equation

$$[A]\{\Delta l\} = \{r\} \tag{6}$$

where $[A] = [U]^T[\bar{U}]$ and $\{r\} = -[U]^T\{\psi\}$. This method is computationally efficient, but it results in a $\Delta l_{\max}$ value that is more than 30 times larger than that of either previous method.

Table 1 provides a more complete comparison between the characteristics of the antenna reflector before and after each shape-control correction method. The results should be compared to the required limits on side lobe level (SLL $\leq G_0 - 30$ dB), gain ($G \geq G_0 - 0.3$ dB), and rms distortion (rms ≤ 0.1690 in.).

Table 1 Results of shape-control optimization

Optimization Method	SLL (wrt G_0), dB	G (wrt G_0), dB	rms, in.	$\Delta l_{\max}$, in.
None	−22.7	−0.64	0.418	0.
Full	−29.7	−0.11	0.168	0.066
rms-limited	−25.9	−0.14	0.172	0.051
Minimum rms	−31.5	−0.02	0.067	2.200
Required	−30.0	−0.30	0.169	—

Refined Electromagnetic Analysis

As mentioned previously, the EM analysis during the optimization procedure calculates SLL at only four azimuth angles. There is a concern that reducing SLL in four discrete directions (i.e., $\phi = 0, 45, 90, 135$ deg) simply allows SLL to increase in other directions. This question is addressed by performing a more detailed EM analysis of the optimized antenna using 41 values of ϕ and comparing it to a similar analysis of the unoptimized antenna.

Figure 7 contains such contours for the original uncorrected antenna (see Fig. 7a), the full optimization solution (Fig. 7b), the rms-limited solution (Fig. 7c), and the minimum rms solution (Fig. 7d). Levels that are higher than -20 dB (wrt G_0) are shaded black. Levels that are between -20 and -25 dB are shaded dark gray. Levels that are between -25 and -30 dB are shaded light gray.

If the full optimization procedure were perfectly successful, then all of the shaded areas in Fig. 7b would remain in the main beam region defined by a circle of radius θ_0. In other words, all relative power levels outside the main beam would be at least 30 dB below G_0. By this criteria, the full optimization solution is not perfectly successful. However, the improvement between the uncorrected antenna and the corrected antenna is very significant. Additional improvement is possible by using more than four azimuthal angles to define the SLL and by adjusting the parameter that controls tolerance to constraint violation.

In contrast with the good results of the full optimization, the rms-limited optimization shows little improvement over the uncorrected antenna. Comparison of Figs. 7a and 7c verifies that simply improving the surface accuracy does not guarantee improvement of EM performance.

As expected, the contour that corresponds to the minimum rms surface distortion (see Fig. 7d) is the best. However, the difference between the contours in Figs. 7b and 7d is not very significant. It is questionable whether this small improvement justifies the increased actuator effort required to attain it.

Concluding Remarks

This paper described the development of an integrated structural-electromagnetic optimization procedure for shape control of orbiting large space antenna reflectors. The procedure employs standard finite-element structural analysis, aperture integration EM analysis, and constrained optimization techniques to predict a set of actuator inputs that will improve antenna performance while minimizing applied control effort. The procedure is tested for a 55-m tetrahedral truss antenna design that has a surface distortion caused by length errors in individual members of the truss. It is shown that the current procedure converges to a much better set of actuator inputs than the traditional approach based on rms surface distortion constraints.

The procedure described in this paper is applicable to a wide variety of large space antenna concepts. The only assumption is that the original surface distortion is precisely known at a discrete number of surface locations and that the change in this distortion for a prescribed change in actuator inputs can be predicted. The quality of the optimum design can be improved by improving the finite-element model of the structure, by increasing the number of discrete points used to describe the surface, and by increasing the number of azimuth angles used to define SLL.

It is concluded that an integrated structures-electromagnetic optimization procedure is highly desirable for static shape control of large space antennas. Indirect approaches that infer antenna performance from rms distortion may be unreliable and can use considerably more control effort than necessary.

References

[1]Lightner, E. B. (ed.), "Large Space Antenna Systems Technology—1982," NASA CP-2269, May 1983.

[2]"Requirements, Design, and Development of Large Space Antenna Structures," AGARD Rept. R-676, May 1980.

[3]Wright, R. L. (ed.), "Microwave Radiometer Spacecraft—A Design Study," NASA RP-1079, Dec. 1981.

[4]Keafer, L. S. and Harrington, R. F., "Radiometer Requirements for Earth-Observation Systems Using Large Space Antennas," NASA RP-1101, June 1983.

[5]Ruze, J., "Antenna Tolerance Theory—A Review," *Proceedings of the IEEE*, Vol. 54, No. 4, Institute of Electrical and Electronics Engineers, Inc., New York, April 1966, pp. 633–640.

[6]Blank, S. J. and Imbriale, W. A., "Array Feed Synthesis for Correction of Reflector Distortion and Vernier Beamsteering," *The Telecommunications and Data Acquisition Report*, edited by E. C. Posner, NASA CR-179715, Aug. 1986, pp. 43–55.

[7]Knight, C. J., Sutton, G. W., and Berggren, R., "Phase Aberrations and Laser Output Beam Quality," *Proceedings of the International Society of Optical Engineering*, Vol. 293, SPIE, Bellingham, WA, Aug. 1981, pp. 2–11.

[8]Adelman, H. M. and Padula, S. L., "Integrated Thermal Structural Electromagnetic Design Optimization of Large Space Antenna Reflectors," NASA TM-87713, June 1986.

[9]Steinbach, R. E. and Winegar, S. R., "Interdisciplinary Design Analysis of a Precision Spacecraft Antenna," AIAA Paper 85-0804, April 1985.

[10]Shu, C. F. and Chang, M.-H., "Integrated Thermal Distortion Analysis for Satellite Antenna Reflector," AIAA Paper 84-0142, Jan. 1984.

[11]Clark, S. C. and Allen, G. E., "Thermo-Mechanical Design and Analysis System for the Hughes 76-Inch Parabolic Antenna," AIAA Paper 82-0864, June 1982.

[12]Greene, W. H., "Effects of Random Member Length Errors on the Accuracy and Internal Load of Truss Antennas," *Journal of Spacecraft and Rockets*, Vol. 22, No. 5, Sept.–Oct. 1985, pp. 554–559.

[13]Haftka, R. T. and Adelman, H. M., "An Analytical Investigation of Shape Control of Large Space Structures by Applied Temperatures," *AIAA Journal*, Vol. 23, March 1985, pp. 450–457.

[14]Haftka, R. T. and Adelman, H. M., "Selection of Actuator Locations for Static Shape Control of Large Space Structures by Heuristic Integer Programming," *Computers and Structures*, Vol. 20, No. 1–3, 1985, pp. 575–582.

[15]Whetstone, W. D., "EISI-EAL Engineering Analysis Language Reference Manual," Engineering Information Systems, Inc., San Jose, CA, 1983.

[16]Rudduck, R. C. and Chang, Y. C., "Numerical Electromagnetic Code—Reflector Antenna Code—NEC-REF (version 2), Part I, User's Manual," Ohio State Univ. ElectroScience Lab., Dept. of Electrical Engineering, Ohio State Univ., Columbus, OH, Rept. 712242-16, Contract N00123-79-C-1469 for Naval Regional Procurement Office, Dec. 1982.

[17]Bailey, M. C., "Hoop Column and Tetrahedral Truss Electromagnetic Tests," NASA CP-2447, Pt. 2, June 1987, pp. 737–746.

[18]Akima, H., "A Method of Bivariate Interpolation and Smooth Surface Fitting for Irregularly Distributed Data Points," *ACM Transactions of Mathematical Software*, Vol. 4, No. 2, June 1978, pp. 148–159.

[19]Croswell, W. F. and Bailey, M. C., "Radiometer Antennas. Chap. 31," *Antenna Engineering Handbook*, edited by Johnson and Jasik, McGraw-Hill, New York, 1984.

[20]Vanderplaats, G. N., "CONMIN—A FORTRAN Program for Constrained Function Minimization—User's Manual," NASA TMX-62282, Aug. 1973.